Astronomy & Astrophysics manuscript no. 14897
May 3, 2011

A new Planetary Nebula in the outer reaches of the Galaxy

K. Viironen[1,2,3], A. Mampaso[1,4], R. L. M. Corradi[1,4], J. E. Drew[5], D. J. Frew[6], C. Giammanco[1,4], R. Greimel[7], T. Liimets[8,9], J. E. Lindberg[8,10], M. Rodríguez[11], L. Sabin[12], S. E. Sale[13,5,14,15], P. A. Wilson[8,16], and A. Zijlstra[17]

[1] Instituto de Astrofísica de Canarias (IAC), C/Vía Láctea s/n, 38200 La Laguna, Tenerife, Spain

[2] Centro Astronómico Hispano Alemán, Calar Alto, C/Jesús Durbán Remón 2-2, E-04004 Almeria, Spain

[3] Centro de Estudios de Física del Cosmos de Aragón (CEFCA), C/General Pizarro 1-1, E-44001 Teruel, Spain
e-mail: kerttu@cefca.es

[4] Departamento de Astrofísica, Universidad de La Laguna, Av. Astrofísico Francisco Sánchez, s/n, 38206 La Laguna, Spain

[5] Centre for Astrophysics Research, University of Hertfordshire, College Lane, Hatfield AL10 9AB, UK

[6] Department of Physics and Astronomy, Macquarie University, North Ryde, NSW 2109, Australia

[7] Institut für Physik, Karl-Franzens Universität Graz, Universitätsplatz 5,8010 Graz, Austria

[8] Nordic Optical Telescope, Ap. 474, E-38700, S/C de La Palma, S/C de Tenerife, Spain

[9] Tartu Observatory, Tõravere, 61602, Estonia

[10] Centre for Star and Planet Formation, Natural History Museum of Denmark, University of Copenhagen, Øster Voldgade 5-7, DK-1350 Copenhagen, Denmark

[11] Instituto Nacional de Astrofísica, Óptica y Electrónica (INAOE), Apdo Postal 51 y 216, 72000 Puebla, Mexico

[12] Instituto de Astronomía UNAM, Km. 103 Carretera Tijuana-Ensenada, C.P. 22860, Ensenada, Baja California, Mexico

[13] Imperial College London, Blackett Laboratory, Prince Consort Road, London SW7 2AZ, UK

[14] Departamento de Física y Astronomía, Facultad de Ciencias, Universidad de Valparaíso, Ave. Gran Bretaña 1111, Playa Ancha, Casilla 53, Valparaíso, Chile

[15] Departamento de Astronomía y Astrofísica, Pontificia Universidad Católica de Chile, Av. Vicuña Mackenna 4860, Casilla 306, Santiago 22, Chile

[16] Institute of Theoretical Astrophysics, University of Oslo, P.O. Box 1029 Blindern, N-0315 Oslo, Norway

[17] Jodrell Bank Centre for Astrophysics, Alan Turing Building, University of Manchester, Manchester, M13 9PL, UK

ABSTRACT

Aims. A proper determination of the abundance gradient in the Milky Way requires the observation of objects at large galactiocentric distances. With this aim, we are exploring the planetary nebula population towards the Galactic Anticentre. In this article, the discovery and physico-chemical study of a new planetary nebula towards the Anticentre direction, IPHASX J052531.19+281945.1 (PNG 178.1-04.0), is presented.
Methods. The planetary nebula was discovered from the IPHAS survey. Long-slit follow-up spectroscopy was carried out to confirm its planetary nebula nature and to calculate its physical and chemical characteristics.
Results. The newly discovered planetary nebula turned out to be located at a very large galactocentric distance (D_{GC} = 20.8±3.8 kpc), larger than any previously known planetary nebula with measured abundances. Its relatively high oxygen abundance (12+log(O/H) = 8.36±0.03) supports a flattening of the Galactic abundance gradient at large galactocentric distances rather than a linearly decreasing gradient.

Key words. planetary nebulae: individual, Galaxy: abundances

1. Introduction

The INT Photometric H-Alpha Survey of the Northern Galactic Plane (IPHAS, Drew et al. 2005; González-Solares et al. 2008) is significantly increasing the number of detected Galactic planetary nebulae (PNe). Viironen et al. (2009a) published a list of 781 new IPHAS PN candidates, whereas the discovery and detailed study of five new IPHAS PNe were presented by Viironen et al. (2009b).

PNe towards the Galactic Anticentre are of special interest as this is where the objects with the largest galactocentric distances are most easily found and studied. Finding new distant PNe will make a crucial contribution to the knowledge of the Galactic abundance gradient, since their rich emission line spectra can yield accurate abundances. The abundance gradient is a topic that is still under debate (see e.g. Maciel & Costa 2009, and references therein). In addition to the shortage of known objects at large galactocentric distances, the main problem is the difficulty of reliably measuring PN distances (see Kwok 2000, for example). The new faint (and therefore potentially distant) IPHAS Anticentre PN candidates combined with new methods for distance determination (Sale et al. 2009; Frew & Parker 2006) can make a significant contribution to the problem.

The location of the newly discovered PN IPHASX J052531.19+281945.1, at only four degrees from the direction of the Galactic Anticentre, motivated us to study this object further. In Sect. 2 the photometric and spectroscopic observations are presented; in Sect. 3 a physical and chemical analysis is carried out; in Sect. 4 its distance is studied; in Sect. 5 a discussion is provided, and in Sect. 6 the main conclusions are presented.

2. Observations and data reduction

The PN was discovered by visually inspecting the IPHAS Hα − r' mosaics of the Anticentre region. The semi-automated searching method described in Viironen et al. (2009a) missed the object due to its relatively large size (∼ 10″). The IAU approved name for this IPHAS object is, after its coordinates, IPHASX J052531.19+281945.1 (X for extended) whereas the IAU common PN name would be PNG 178.1-04.0. To abbreviate, in the following we will use the acronym IACPN (IPHAS Anti-Centre Planetary Nebula).

2.1. IPHAS imaging

The IPHAS observations of IACPN were carried out on November 2003 using the 2.5m Isaac Newton Telescope and its Wide Field Camera under seeing condition of 1.3″ FWHM in the Hα images. Fig. 1 presents the Hα, r' and i' images of the object. The exposure times are 120 s for Hα and 10 s for r' and i' images. More details about IPHAS observations and the data reduction are given in Drew et al. (2005) and González-Solares et al. (2008).

IACPN shows a roughly spherical morphology. It is hardly visible in the IPHAS i' filter (see Fig. 1). No objects are listed in SIMBAD within almost 5′ from the position of IACPN.

2.2. SPM 2.1-m spectroscopy

The first spectroscopic observations of IACPN were carried out at the Observatorio de San Pedro Mártir (Mexico), and were presented by Mampaso et al. (2005) in a conference paper. Four 20 min exposures in the red and five 20 min exposures in the blue were obtained through a narrow (1″) slit using the 2.1-m telescope and the B&Ch spectrograph (2 Å pix^{-1} dispersion, 3 Å resolution, from 3720 to 7470 Å). In addition, two 10 min exposures in the blue were obtained with a very wide slit in order to include the whole nebula and measure its total Hβ flux. Furthermore, the MEZCAL echelle spectrograph was used with the same telescope to obtain a high dispersion spectrum (0.1 Å pix^{-1}) around the Hα line.

The MEZCAL spectrum allowed to measure the expansion and radial velocities of the nebula: the ∼10″diameter shell has a radial velocity of v_{LSR} = 13.5 km s^{-1} and expands at 17 km s^{-1} in the [N II] 6583 Å line (Mampaso et al. 2005). From the B&Ch spectra the PN nature of the nebula was confirmed and its absolute Hβ flux was measured, giving F(Hβ) = 3.34 × 10^{-14} erg cm^{-2} s^{-1}. Preliminary chemical abundances were presented by Mampaso et al. (2005).

2.3. WHT + ISIS spectroscopy

The William Herschel Telescope (WHT) + ISIS spectrograph observations of IACPN were carried out in service mode on April 6, 2007. The seeing was ∼ 0.9″ and the weather conditions were good, except for the presence of light cirrus during the second half of the night. Three exposures of 20 min of the target were obtained in both the blue (3570-5115 Å; dispersion 0.8 Å pix^{-1}, resolution 3.2 Å) and the red (5540-10500 Å, 1.8 Å pix^{-1} dispersion, 6.5 Å resolution) arms with the slit located at P.A. = 79^o, i.e. at the parallactic angle corresponding to the moment of observation. The slit width was 1″. In addition, bias, lamp flats, and arc exposures were obtained. Unfortunately, no suitable observations of spectrophotometric standards are available for that night, as all standard stars were observed with a different instrumental configuration than our target. For this reason, a spectrum of the standard star BD+332642 (Oke 1990), obtained on April 2, 2007 with the same setup as for the nebula, was used to flux calibrate its spectrum. Nevertheless, the blue and red observations of this standard star were obtained at different times of the night, and therefore under different weather conditions. This prevents a precise matching of the blue and red sides of the WHT spectrum, and therefore, an accurate determination of A_V using the Hα/Hβ flux ratio. For this reason, additional spectra of the nebula and standard star were acquired as described below. Finally, and given that there is calibration data available for BD+33 2642 only up to 9200 Å (Oke 1990), the fluxes for lines at longer wavelengths will not be considered. The data reduction and calibration were carried out using the standard IRAF routines for longslit spectroscopy.

2.4. NOT + ALFOSC spectroscopy

A good measurement of the reddening of the nebula, A_V, is important for its distance determination (see Sec. 4) and additional spectra of IACPN were secured in service mode on September 6, 2010 using the ALFOSC instrument at the Nordic Optical Telescope. These spectra were obtained so as to cover the wavelength range from ∼3800 Å to 6800 Å, i.e. to include simultaneously the main Balmer lines (Hδ, Hγ, Hβ, and Hα). The night was photometric and the seeing was 0.7″. Two 20 min exposures were obtained. The spectral dispersion was 1.5 Å pix^{-1} and resolution 6 Å. The slit was positioned according to the parallactic angle at the moment of observation (P.A. = 102^o) and

Send offprint requests to: K. Viironen

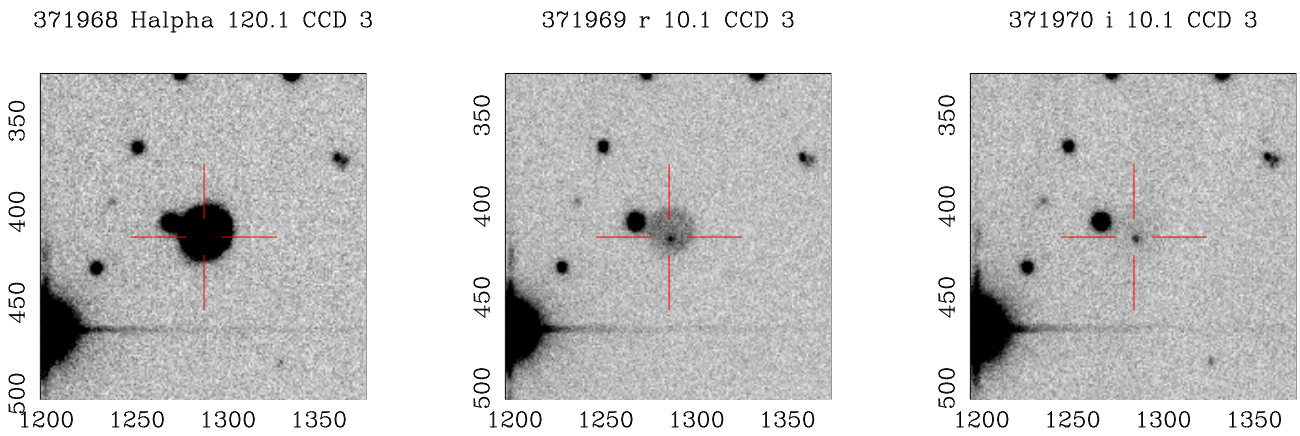

Fig. 1. IPHAS Hα, r' and i' discovery images of IACPN, from left to right. The image sizes are $1' \times 1'$, North is up and East to the left.

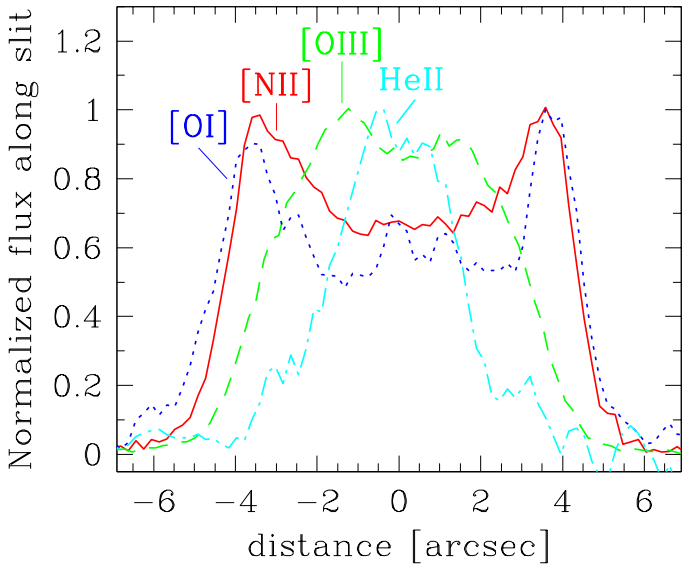

Fig. 2. Spatial profiles extracted from the NOT spectrum for representative lines from ions with different ionisation potentials.

the slit width used was 1″. Bias, lamp flats, and arc exposures were obtained, and the standard star G191-B2B was observed. The data reduction and calibration were carried out using the standard IRAF routines for longslit spectroscopy.

3. Spectroscopic analysis

The spatial distribution of the emission from several lines in the NOT spectrum is presented in Fig. 2, and shows that IACPN exhibits a strong ionisation stratification, with higher excitation emissions coming from regions progressively closer to the centre. For this reason, care has to be exercised when comparing line fluxes from the WHT and NOT spectra. The difference in slit P.A. for both datasets is relatively small (23^o) and the spatial profiles for the WHT spectrum (not shown here) are very similar to those of the NOT (Fig. 2) a likely consequence of the round symmetry of the object. On the other hand, in the WHT data the slit passes through the star partly overlapping the nebula on its eastern side (see Fig. 1), and special care was taken to extract this star from the nebular spectrum.

A one-dimensional spectrum of the object (both from the WHT and the NOT data) was extracted summing the nebular spectra along the spatial axis. The WHT spectrum is shown in Fig. 3.

Line fluxes were measured fitting Gaussian profiles using the task SPLOT of IRAF. The errors in the line fluxes were calculated considering both the statistical errors and errors due to the flux calibration. The latter were obtained for each line from the error in the calibration data at the wavelength under question and the local RMS of the fitted calibration curve, and were added quadratically to the statistical errors. Resulting line fluxes are listed in Tables 1 (WHT) and 2 (NOT); fluxes in common in both datasets were found to agree within 3-σ, and in most cases within 1-σ. The WHT line fluxes were used in the physico-chemical analysis that follows.

3.1. Reddening

The reddening law of Fitzpatrick (2004) for $R_V = 3.1$, and the Balmer line fluxes from Tables 1 and 2 were used to derive the extinction coefficient c_β from both the WHT and NOT spectra. For the WHT data, we derive $c_{H\beta} = 0.7 \pm 0.1$ and 0.9 ± 0.1 from the Hγ/Hβ and Hδ/Hβ line ratios, respectively. For the NOT, very similar values are obtained, namely $c_{H\beta} = 0.8 \pm 0.1, 0.7 \pm 0.2$, and 0.6 ± 0.2 from the Hα/Hβ, Hγ/Hβ, and Hδ/Hβ ratios, respectively. The weighted mean of all measurements is $c_{H\beta} = 0.8 \pm 0.1$, i.e. $A_V = 1.7 \pm 0.2$.

We have adopted this value to deredden the NOT spectrum and, separately, the blue and red WHT spectra of the nebula. Given the lack of a precise match of the blue and red parts in the WHT data (Sect. 2.4) a final correction to these data was applied after dereddening by rescaling the whole red spectrum to match the theoretical value $I(\mathrm{H}\alpha)/I(\mathrm{H}\beta) = 2.86$ (Osterbrock 1974).

The extinction derived in this paper is within the errors, albeit slightly larger, than the value from Mampaso et al. (2005), $A_V = 1.5 \pm 0.2$ mag (derived from a noiser Hα/Hβ ratio and using a different extinction law).

3.2. Density and temperature

The IRAF package TEMDEN was used to derive the electronic density and temperature. The density was derived by iterating the density calculated from the [S II]6716 Å/6731 Å line ratio and the temperature derived from the [N II](6548 Å+6583 Å)/5755 Å line ratio. This leads to N_e =190±120 cm^{-3}, when the errors in the dereddened sulphur line fluxes are considered. The density

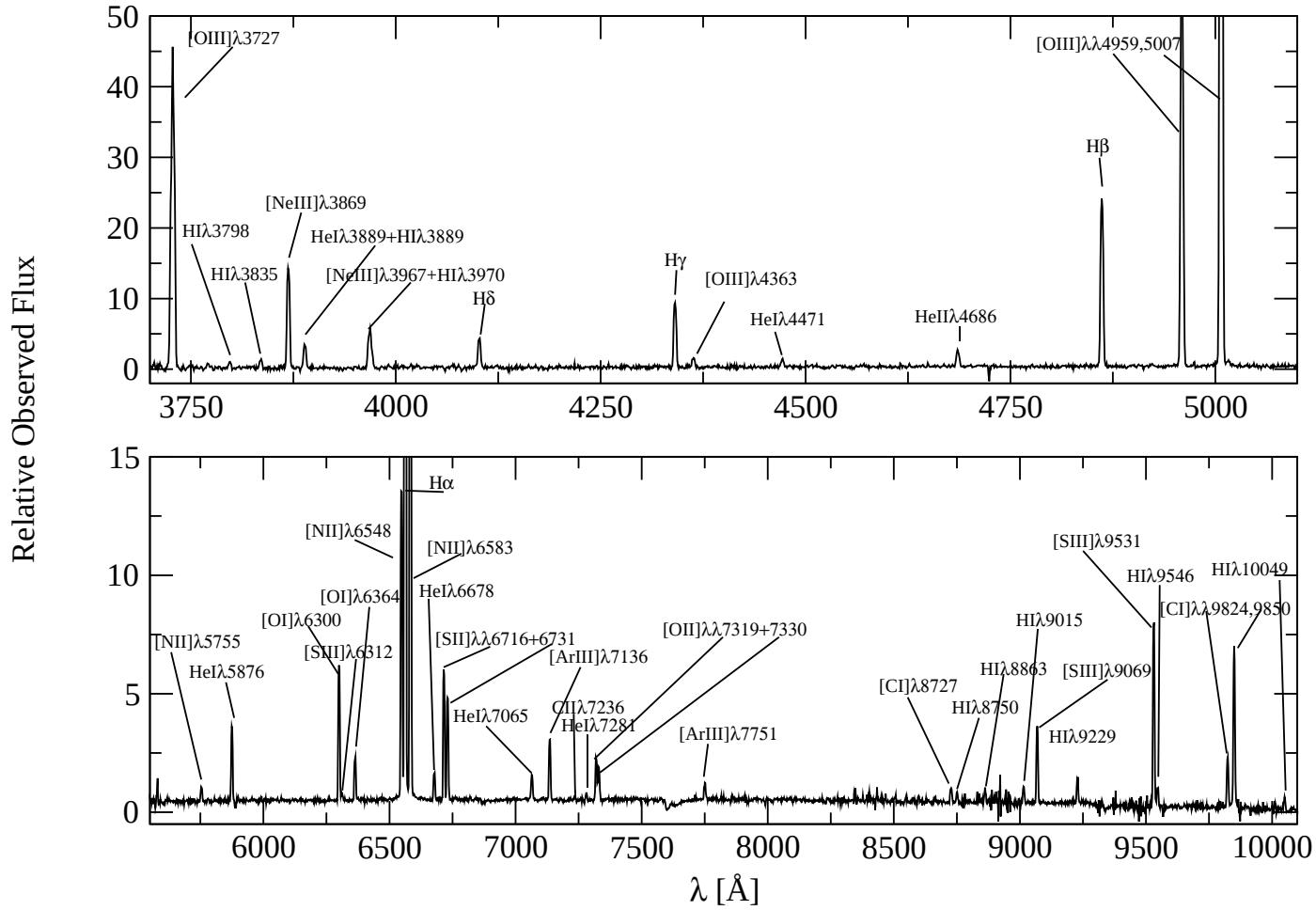

Fig. 3. The WHT+ISIS spectrum of IACPN.

error is large as the [S II]6716 Å/6731 Å line ratio is at the upper limit of its usability for the N_e determination.

Adopting the [S II] density, the electronic temperature was derived from [N II](6548 Å+6583 Å)/5755 Å, [O II](3726 Å+3729 Å)/(7320 Å+7330 Å), and [O III](4959 Å+5007 Å)/4363 Å line ratios giving, respectively, 11700±800 K, 12000±800 K, and 11700±300 K.

3.3. Chemical abundances

The ionic abundances of He^+ and He^{++} and corresponding errors were calculated using the equations of Benjamin et al. (1999) which include the effects of collisional excitation on He I lines. The ionic abundances for the rest of the elements were calculated using the NEBULAR analysis package in IRAF/STSDAS (Shaw & Dufour 1994). For the ions with the lowest ionisation potentials, O^+ ([O II] 3727 Å, 7319 Å, 7330 Å), N^+ ([N II] 5755 Å, 6548 Å, 6583 Å), and S^+ ([S II] 6716 Å+ 6731 Å) the T_e[N II] was adopted, while for the higher ionisation potential ions, He^+ (He I 4471 Å, 5876 Å, 6678 Å), He^{++} (He II 4686 Å), O^{++} ([O III] 4363 Å, 4959 Å, 5007 Å), Ne^{++} ([Ne III] 3869 Å), S^{++} ([S III] 6312 Å, 9069 Å), and Ar^{++} ([Ar III] 7135 Å, 7751 Å), the T_e[O III] was used. The [S II] density was adopted for all the ions. The errors were calculated using the Monte Carlo method, assigning for each variable (flux, temperature, and density) 100 random values within a normal distribution defined by the corresponding quantity and its 1-σ uncertainty and calculating the resulting RMS in the ionic abundance. The ionic abundances derived from different lines of the same ion agree within 1.5σ in all cases. The total elemental abundances were then determined by applying ionisation correction factors (ICFs) following the prescriptions by Kingsburgh & Barlow (1994), and the errors were propagated to include the ionic abundance errors derived above and the errors in the ICF's. The ionic and total abundances with their corresponding errors are given in Table 3.

4. Distance

The distance to IACPN was estimated using two different methods.

Firstly, we used the extinction–distance technique ($A_v - D$; c.f. Gathier et al. 1986) as implemented by Sale et al. (2009) for IPHAS data. The $A_v - D$ method is currently the only one which is capable of determining accurate ($\sim$ 30%) distances for a large number of PNe, being independent of statistical assumptions about the physics of the nebulae and/or of their central stars (Giammanco et al. 2011). GAIA will hopefully improve this situation in the near future by providing hundreds of trigonometric PN distances. The $A_v - D$ curve towards the sightline of IACPN (l, b = 178.13, −4.04) was calculated using photometry of 3629 stars in a 10′ × 10′ box centred on the position of the PN and is shown in Fig. 4. Most of the interstellar extinction builds up within the first kiloparsec, beyond which it remains roughly constant at $A_V \sim 2$. We note that this behaviour is consistent with

Table 1. WHT+ISIS observed line fluxes F (Obs.) normalised to F(Hβ) = 100 in the blue section of the spectrum (separated by a horizontal line) and to F(Hα) = 100 in the red section. See text for details about the normalisation of the dereddened fluxes, F (deredd). The wavelengths are in units of Å and the total errors in the flux measurements and the propagated errors in the dereddened flux are given within brackets in percentage.

Line, λ	λ Obs.	F (Obs.)	F (deredd)
[O II] 3726.03+3728.82	3727.8	213.7 (2)	379.9 (7)
H I 3797.90	3797.4	2.8 (15)	4.8 (16)
H I 3835.39	3835.3	4.4 (10)	7.5 (11)
[Ne III] 3868.75	3868.9	57.1 (2)	94.8 (6)
He I 3888.65 + H I 3889.05	3889.0	13.3 (4)	21.9 (7)
[Ne III] 3967.46+H I3970.07	3968.4	28.1 (3)	44.4 (6)
Hδ 4101.74	4101.8	17.0 (4)	25.2 (6)
Hγ 4340.47	4340.7	36.8 (2)	47.9 (4)
[O III] 4363.21	4363.2	5.4 (8)	6.9 (8)
He I 4471.50	4471.7	4.1 (11)	5.0 (12)
He II 4685.68	4685.7	9.6 (7)	10.5 (7)
Hβ 4861.33	4861.6	100.0 (2)	100.0 (2)
[O III] 4958.91	4959.1	238.6 (2)	227.7 (2)
[O III] 5006.84	5007.1	728.9 (1)	680.0 (2)
[N II] 5754.64	5754.1	0.8 (11)	3.1 (12)
He I 5875.64	5875.1	4.4 (3)	15.9 (5)
[O I] 6300.30	6299.9	8.1 (2)	24.9 (7)
[S III] 6312.10	6312.0	0.4 (16)	1.2 (18)
[O I] 6363.78	6363.4	2.7 (3)	8.1 (7)
[N II] 6548.03	6547.5	18.6 (1)	53.4 (7)
Hα 6562.82	6562.2	100.0 (1)	286.0 (7)
[N II] 6583.41	6582.8	55.5 (1)	157.7 (7)
He I 6678.15	6677.6	1.7 (5)	4.7 (9)
[S II] 6716.47	6715.9	7.6 (1)	20.9 (8)
[S II] 6730.85	6730.4	6.2 (2)	16.8 (8)
He I 7065.28	7064.8	1.5 (3)	3.8 (9)
[Ar III] 7135.78	7135.4	3.6 (2)	8.9 (9)
C II 7236.42	7235.0	0.2 (28)	0.5 (30)
He I 7281.35	7280.8	0.3 (23)	0.8 (24)
[O II] 7318.39+7319.99	7319.5	2.4 (3)	5.7 (10)
[O II] 7329.66+7330.73	7329.9	2.1 (4)	5.0 (10)
[Ar III] 7751.10	7750.7	1.0 (9)	2.1 (14)
[C I] 8727.13	8727.1	1.0 (8)	1.8 (15)
H I 8750.47	8750.7	0.5 (14)	1.0 (18)
H I 8862.79	8861.9	0.6 (21)	1.0 (24)
H I 9014.91	9014.8	1.0 (18)	1.8 (22)
[S III] 9068.9	9068.7	4.5 (2)	7.8 (13)

Table 2. As in Table 1 for the NOT spectrum normalised to F(Hβ)=100.

Line, λ	λ Obs.	F (Obs.)	F (deredd)
[Ne III] 3868.75	3868.7	61.8 (9)	101.8 (11)
He I 3888.65 + H I 3889.05	3889.2	13.8 (25)	22.4 (26)
[Ne III] 3967.46+H I3970.07	3967.5	29.6 (10)	46.4 (12)
Hδ 4101.74	4101.5	19.3 (10)	28.4 (11)
Hγ 4340.47	4340.2	37.0 (5)	48.0 (6)
He II 4685.68	4685.2	11.3 (11)	12.3 (11)
Hβ 4861.33	4860.9	100.0 (2)	100.0 (2)
[O III] 4958.91	4958.4	243.8 (2)	232.9 (2)
[O III] 5006.84	5006.4	742.1 (1)	693.2 (2)
[N II] 5754.64	5754.8	4.4 (21)	3.0 (22)
He I 5875.64	5874.8	22.1 (5)	14.5 (7)
[O I] 6300.30	6299.8	41.7 (5)	23.7 (9)
[S III] 6312.10	6310.6	2.5 (57)	1.4 (58)
[O I] 6363.78	6362.7	14.5 (7)	8.1 (11)
[N II] 6548.03	6546.9	96.5 (4)	51.0 (9)
Hα 6562.82	6561.8	553.9 (4)	291.3 (9)
[N II] 6583.41	6582.5	311.4 (4)	162.7 (9)
He I 6678.15	6677.3	8.4 (18)	4.3 (20)
[S II] 6716.47	6715.2	37.7 (5)	19.0 (10)
[S II] 6730.85	6729.5	29.4 (5)	14.7 (11)

Table 3. Ionic and total abundances for IACPN. The percentage errors are given within brackets.

Ion/Element	Abundance	12+log(X/H)
He I	0.117 (10)	
He II	0.009 (7)	
He/H	**0.125 (9)**	**11.10±0.04**
[O II]	7.69E-5 (4)	
[O III]	1.42E-4 (2)	
icf(O)	1.05 (8)	
O/H	**2.30E-4 (7)**	**8.36±0.03**
[N II]	2.07E-05 (0.2)	
icf(N)	2.99 (8)	
N/H	**6.20E-05 (8)**	**7.79±0.03**
[Ar III]	5.72E-07 (1)	
icf(Ar)	1.87 (22)	
Ar/H	**1.07E-06 (22)**	**6.03±0.10**
[S II]	6.14e-07 (18)	
[S III]	1.50E-06 (3)	
icf(S)	1.12 (1)	
S/H	**2.37E-06 (6)**	**6.37±0.02**
[Ne III]	5.26E-05 (12)	
icf(Ne)	1.62 (7)	
Ne/H	**8.50E-05 (14)**	**7.93±0.06**

the extinction map of Schlegel et al. (1998) which gives an integrated Galactic extinction of $A_V = 1.9$ towards this sightline, i.e. close to the asymptotic value shown by Fig. 4. The likely reason for such an abrupt asymptoting is that, at the distance of the Perseus arm (the only major dusty structure encountered beyond 1 kpc along this line of sight), a Galactic latitude of $b = -4.04°$ corresponds to a distance of $\sim$ 140 pc below the midplane, and little cumulative dust obscuration is expected farther out.

According to Fig. 4, IACPN could be located at any distance from <1 kpc (the formal best fit to the uprising section of the curve) to $\gtrsim$8 kpc (the limit where there are adequate stellar data). The error bars of the stellar and the PN data overlap at 2σ and the plateau of interstellar extinction along this line of sight precludes a thrustworthy estimation of the extinction distance to this PN.

Secondly, the relationship between Hα-surface brightness and nebular radius ($S - r$) of Frew & Parker (2006, 2010) was used. IACPN is almost circular, and its dimensions, measured directly from the Hα IPHAS image at the 10 percent of peak-brightness contour, following the procedure of Tylenda et al. (2003), are 10.5×9.7 arcsec.

The total Hα flux was calculated from the wide-slit Hβ flux (Section 2.2) and the Balmer decrement of 5.5 ± 0.2, resulting in log F(Hα) = -12.73 ± 0.05. The Hα flux was also independently estimated from the IPHAS calibrated Hα image after subtracting the contribution of the two adjacent [N II] lines as measured form the spectrum, yielding log F(Hα) = -12.96 ± 0.22, in fair agreement with the spectroscopically determined value. We will adopt the better determined spectroscopic value in the following.

The resulting Hα surface brightness is log S(Hα) = -4.00 ± 0.06 erg cm^{-2} s^{-1} sr^{-1}. After dereddening this value using $A_V = 1.7 \pm 0.2$ mag and the extinction law of Fitzpatrick (2004) with $R_V = 3.1$, we find the physical radius of the PN to be 0.31 pc, using the mean Hα $S - r$ relation of Frew & Parker (2006). The mean-trend equation (Frew 2008, Frew et al. 2011, in prepara-

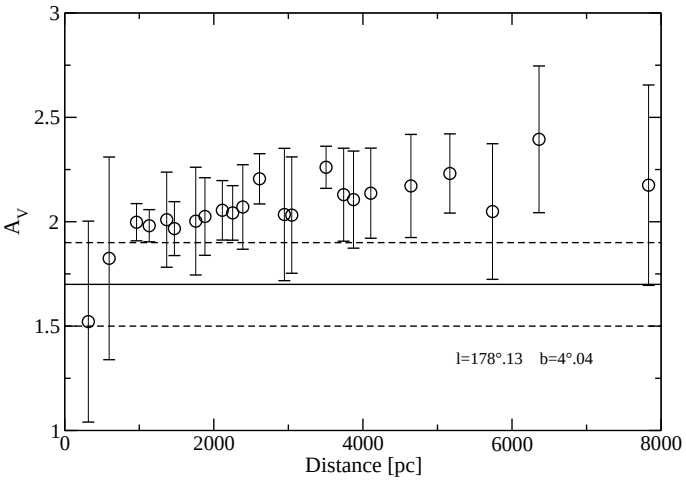

Fig. 4. IPHAS extinction – distance curve (circles) for field stars towards the sightline of IACPN. The horizontal line shows the measured extinction A_V of IACPN flanked by two dashed lines representing $\pm 1\sigma$ error limits.

tion) was used, which is applicable to round, optically-thick PN, viz.:

$$\log S(\mathrm{H}\alpha) = -3.65(\pm 0.08)\log R - 5.34(\pm 0.07). \quad (1)$$

The resulting distance is 12.8 ± 3.7 kpc. The quoted uncertainty in the distance includes the formal dispersion of the relation (± 28%; Frew 2008) which is the dominant error term, added in quadrature with the estimated uncertainties of the integrated Hα flux, mean diameter, and reddening of the PN. The corresponding galacto-centric distance is D_{GC} = 20.8 ± 3.8 kpc if a distance to the Sun of 8.0 ± 0.6 kpc (Ghez et al. 2008) is assumed. At 12.8 kpc from the Sun, IACPN is located about 1 kpc off the plane of the Galactic disk. That is a large height indeed, but we note that the well-known flaring of the outer disk (see e.g. Gyuk et al. 1999) allows a high probability of thin disk objects being located even at this offset from the mid-plane. Using the Gyuk et al. (1999) prescription, the thin disk scale height at D_{GC} = 20.8 kpc is in excess of 1 kpc (even if the solar neighbourhood scale height is reduced in line with the Jurić et al. (2008) result).

We will adopt for IACPN the $S - r$ distance of 12.8 kpc. At D_{GC}=20.8 kpc, it would be one of the most distant planetary nebula from the Galactic Centre for which a distance has been determined (c.f. Acker et al. 1994; Stanghellini et al. 2008) and the farthest PN from the Galactic Centre with measured abundances (Maciel & Costa 2009; Henry et al. 2010).

5. Discussion

IACPN is a low density planetary nebula with an emission line spectrum typical of a moderate excitation Type II PN (Class 3 of Dopita & Meatheringham 1990). This, together with its strong stratification, apparent from He II to O I (Fig. 2), suggests that it is composed of a moderately massive nebula hosting a relatively hot star. The ionised hydrogen mass of the nebula, derived from its Hβ flux, electron temperature, radius, and distance, is M= 0.4 $M_\odot$. The nebular expansion velocity (17 km s^{-1}) and the physical radius (0.31 pc at the distance of 12.8 kpc) lead to a kinematic age of 17800 yr. Such a large kinematical age would point to a low mass central star if a luminosity larger than $\sim 300 - 500$ $L_\odot$ is required (cf. Blöcker 1995). To crudely estimate the central star mass, we follow the prescriptions of Maciel et al. (2010) for a N/O abundance ratio as given in Table 3, finding m_{cs} = 0.6 $M_\odot$ and an age for the progenitor star of ∼4 Gyr (if Case A from Maciel et al. 2010 is assumed). However, given the several uncertain parameters involved (central star luminosity and temperature, kinematical vs. real age), no precise estimate of the stellar mass can be derived.

We have ran several simple Cloudy (Ferland et al. 1998) photoionisation models using spherical or shell geometry and the model atmospheres of Rauch (2003). We assumed a nebula with an outer radius of 0.31 pc, hydrogen density of 200 cm^{-3}, and chemical abundances 0.3 dex below those labelled in Cloudy as "planetary nebula". This implies that the input models have 12+log(O/H)=8.34 and He/H=0.1, close to our measured values. On the other hand, the model abundances of N, Ar, and S are 0.1-0.3 dex above our derived values, whereas the model abundance of Ne is 0.2 dex below the value listed in Table 3. Since the abundances of these elements are more uncertain, and since our comparison is based on the He and O ions, this should be a good approximation for our purposes. We considered the observed intensities of the He I, He II, [O I], [O II], and [O III] lines, as given in Table 1, and found that high stellar temperatures ($T_{eff} \gtrsim 10^5$ K) are needed to account for the observed intensity of the He II 4686 Å line, in agreement with the results presented above. Models with those effective temperatures also reproduce the intensities of all the aforementioned lines. The radiation-bounded case requires a luminosity for the ionising source $L_{cs} \sim 100$ $L_\odot$, being therefore consistent with a low mass star on the cooling track. As a matter of fact, similar models for radiation-bounded nebulae as small as 0.01 pc (corresponding to extinction distances smaller than 1 kpc; see Section 4) would imply central star luminosities around 0.001 $L_\odot$, i.e., much lower than the expected luminosity range of 10-1000 $L_\odot$ for stars on the cooling track. This renders implausible models using very short distances for this PN.

We also investigated the [O III] luminosity of IACPN to compare it to the bright-end cutoff of the PN luminosity function (PNLF: Ciardullo 2010). We used the long-slit integrated Hβ flux and the [O III]/Hβ ratio of 7.3 to derive an integrated [O III] flux, $F(5007) = 2.43 \times 10^{-13}$ erg cm^{-2} s^{-1}. Correcting for extinction, and following Jacoby (1989), we derive a PN absolute magnitude, $M_{5007} = +0.3^{+0.7}_{-0.6}$ at the adopted distance. The PN is thus ∼4.8 magnitudes down the PNLF from the bright cut-off magnitude, $M^* = -4.48$. This is consistent with the evolved nature of the PN, and the position of the (unobserved) central star on the WD cooling track.

In summary, all physical data at hand on IACPN are consistent with a distant, aged, radiation-bounded Type II planetary nebula excited by a low mass central star with relatively high temperature and having already reached its cooling track.

With respect to the chemistry, the O/H abundance of 8.36±0.03 (Table 3) is interestingly high for the large galactocentric distance, 20.8 kpc, and makes IACPN a key target for studies of the abundance gradient in the Milky Way. It is generally agreed that there is *some* negative PNe metallicity gradient but the consensus seems to finish there. Values for the best measured element, oxygen, range from $\Delta\log(\mathrm{O/H})/D_{GC} = -0.01$ (Pottasch & Bernard-Salas 2006) to −0.08 (Stanghellini et al. 2006) with most recent values still disagreeing by a factor of two, well above the uncertainties quoted by the authors: c.f. -0.023 ± 0.006 and -0.058 ± 0.006 from Stanghellini & Haywood (2010) and Henry et al. (2010), respectively. Similar confusion hampers the possible existence of a variable slope, i.e. if the gradient steepens (Stanghellini & Haywood 2010) or flattens (Maciel & Costa 2010) outwards along the Galactic equatorial plane, and also on its secular temporal behaviour, either

null (Henry et al. 2010) or steeping (Stanghellini & Haywood 2010) or flattening with time (Maciel & Costa 2010). Perhaps the most sensible conclusion comes from Henry et al. (2010): "Essentially we have reached a confusion limit regarding the abundance gradient as derived using PNe.". One of the major sources of this confusion is the unsettled PNe distance determination problem allied with the extreme paucity of nebulae at large galactocentric distances. In fact, in the most recent works, those by Henry et al. (2010) and Stanghellini & Haywood (2010), only two PNe with $D_{GC} > 17kpc$ are included in each sample (K3-64, K3-70, and M1-9, K3-66, respectively), all four PNe having mediocrily determined O abundances (quoted errors from 0.2 to 0.5 dex) and distances. However, these distant nebulae are obviously critical for the gradient determination.

In this context, IACPN provides a valuable data point located at the outer reaches of the Galaxy, and its well-constrained O abundance do support models with a flatter gradient toward the external disk. An intriguing possibility is that IACPN and perhaps also the other four PNe with D_{GC} >17 kpc might even have an extragalactic origin, if indeed the Monoceros Ring proposed to be located at these radii (eg. Conn et al. 2008) is attributable to a satellite accretion event. A consensus on this has not yet been reached (eg. Hammersley & Lopez-Corredoira 2010). But either way it is clear that the properties of the outer Galactic disc are still in need of much better observational definition.

6. Conclusions

We are exploring the new IPHAS planetary nebula candidates (Viironen et al. 2009a) towards the Galactic Anticentre in order to better sample the Galactic abundance gradient at large galactocentric distances. In this paper, the discovery of a new PN located at only 4 degrees from the Galactic Anticentre, IPHASX J052531.19+281945.1, is presented, its physical and chemical properties are studied and its distance determined. The object turned out to be a low-density, distant, and aged PN. It is the Galactic PN with the largest galactocentric distance (20.8±3.8 kpc) where the chemical abundances have been measured, and this, combined with its relatively high oxygen abundance, 12 + log(O/H) = 8.36±0.03, points to a flattening of the Galactic abundance gradient towards the outer Galaxy rather than to a linearly decreasing oxygen abundance (e.g. Maciel & Costa 2009, and references therein).

To properly study the behaviour of the abundance gradient at the outer Galaxy, reasonably accurate abundance measurements on a sample of objects at large galactocentric distances are needed. We have recently discovered in the IPHAS images about 180 new faint PN candidates located in a $30^\circ \times 10^\circ$ region around the Anticentre (Viironen et al. 2009a). Further abundance measurements of confirmed candidates in this region would help to build a robust chemical gradient determination and reach firmer conclusions concerning its flattening.

Acknowledgements. This paper makes use of data obtained as part of IPHAS carried out at the INT, as well as WHT, NOT/ALFOSC and SPM2.1m spectroscopic data. The INT and WHT are operated by the Isaac Newton Group, whereas NOT is operated jointly by Denmark, Finland, Iceland, Norway, and Sweden, both are at the island of La Palma in the Spanish Observatorio del Roque de los Muchachos of the Instituto de Astrofísica de Canarias. ALFOSC is owned by the Instituto de Astrofísica de Andalucia (IAA) and operated at the NOT under agreement between IAA and the NBIfAFG of the Astronomical Observatory of Copenhagen. SPM 2.1m is operated by UNAM at the OAN of SPM, Mexico. All IPHAS data are processed by the Cambridge Astronomical Survey Unit, at the Institute of Astronomy in Cambridge. L. Sabin is grateful for receiving a UNAM postdoctoral fellowship and is partially supported by PAPIIT-UNAM grant IN109509 (Mexico). Support for S. E. Sale is provided by MIDEPLAN's Programa Inicativa Científica Milenio through grant P07-021-F, awarded to The Milky Way Millennium Nucleus. We thank J. A. López and H. Riesgo for kindly acquiring and reducing the SPM MEZCAL spectra for us, NOT staff (Pilar Montañés Rodríguez, Tapio Pursimo) for obtaining the NOT spectrum, and Q. A. Parker for discussions. Finally, we thank the anonymous referee for helping us to substantially improve the article.

References

Acker, A., Ochsenbein, F., Stenholm, B., et al. 1994, VizieR Online Data Catalog, 5084
Benjamin, R. A., Skillman, E. D., & Smits, D. P. 1999, ApJ, 514, 307
Blöcker, T. 1995, A&A, 299, 755
Ciardullo, R. 2010, PASA, 27, 149
Conn, B. C., Lane, R. R., Lewis, G. F., et al. 2008, MNRAS, 390, 1388
Dopita, M. A. & Meatheringham, S. J. 1990, ApJ, 357, 140
Drew, J. E., Greimel, R., Irwin, M. J., et al. 2005, MNRAS, 362, 753
Ferland, G. J., Korista, K. T., Verner, D. A., et al. 1998, PASP, 110, 761
Fitzpatrick, E. L. 2004, in Astronomical Society of the Pacific Conference Series, Vol. 309, Astrophysics of Dust, ed. A. N. Witt, G. C. Clayton, & B. T. Draine, 33
Frew, D. J. 2008, PhD thesis (Macquarie University)
Frew, D. J. & Parker, Q. A. 2006, in IAU Symposium, Vol. 234, Planetary Nebulae in our Galaxy and Beyond, ed. M. J. Barlow & R. H. Méndez, 49–54
Frew, D. J. & Parker, Q. A. 2010, PASA, 27, 129
Gathier, R., Pottasch, S. R., & Pel, J. W. 1986, A&A, 157, 171
Ghez, A. M., Salim, S., Weinberg, N. N., et al. 2008, ApJ, 689, 1044
Giammanco, C., Sale, S. E., Corradi, R. L. M., et al. 2011, A&A, 525, A58+
González-Solares, E. A., Walton, N. A., Greimel, R., et al. 2008, MNRAS, 707
Gyuk, G., Flynn, C., & Evans, N. W. 1999, ApJ, 521, 190
Hammersley, P. L. & Lopez-Corredoira, M. 2010, ArXiv e-prints
Henry, R. B. C., Kwitter, K. B., Jaskot, A. E., et al. 2010, ApJ, 724, 748
Jacoby, G. H. 1989, ApJ, 339, 39
Jurić, M., Ivezić, Ž., Brooks, A., et al. 2008, ApJ, 673, 864
Kingsburgh, R. L. & Barlow, M. J. 1994, MNRAS, 271, 257
Kwok, S. 2000, The Origin and Evolution of Planetary Nebulae (Cambridge ; New York : Cambridge University Press, 2000. (Cambridge astrophysics series ; 33))
Maciel, W. J. & Costa, R. D. D. 2009, in IAU Symposium, ed. J. Andersen, J. Bland-Hawthorn, & B. Nordström, Vol. 254, 38
Maciel, W. J. & Costa, R. D. D. 2010, in IAU Symposium, ed. K. Cunha, M. Spite, & B. Barbuy, Vol. 265, 317–324
Maciel, W. J., Costa, R. D. D., & Idiart, T. E. P. 2010, A&A, 512, A19+
Mampaso, A., Viironen, K., Corradi, R. L. M., et al. 2005, in American Institute of Physics Conference Series, Vol. 804, Planetary Nebulae as Astronomical Tools, ed. R. Szczerba, G. Stasińska, & S. K. Gorny, 14–14
Oke, J. B. 1990, AJ, 99, 1621
Osterbrock, D. E. 1974, Astrophysics of gaseous nebulae (W. H. Freeman and Co., 1974. 263 p.)
Pottasch, S. R. & Bernard-Salas, J. 2006, A&A, 457, 189
Rauch, T. 2003, A&A, 403, 709
Sale, S. E., Drew, J. E., Unruh, Y. C., et al. 2009, MNRAS, 392, 497
Schlegel, D. J., Finkbeiner, D. P., & Davis, M. 1998, ApJ, 500, 525
Shaw, R. A. & Dufour, R. J. 1994, in Astronomical Society of the Pacific Conference Series, Vol. 61, Astronomical Data Analysis Software and Systems III, ed. D. R. Crabtree, R. J. Hanisch, & J. Barnes, 327
Stanghellini, L., Guerrero, M. A., Cunha, K., Manchado, A., & Villaver, E. 2006, ApJ, 651, 898
Stanghellini, L. & Haywood, M. 2010, ApJ, 714, 1096
Stanghellini, L., Shaw, R. A., & Villaver, E. 2008, ApJ, 689, 194
Tylenda, R., Siódmiak, N., Górny, S. K., Corradi, R. L. M., & Schwarz, H. E. 2003, A&A, 405, 627
Viironen, K., Greimel, R., Corradi, R. L. M., et al. 2009a, A&A, 504, 291
Viironen, K., Mampaso, A., Corradi, R. L. M., et al. 2009b, A&A, 502, 113